Investigating methods to quantifying uncertainty in $PM_{2.5}$ emission rates from cooking by toasting bread

Constanza Molina [a], Benjamin Jones [b,*], Catherine O'Leary [c]

[a] *Escuela de Construcción Civil, Pontificia Universidad Católica de Chile, Santiago, Chile*
[b] *Department of Architecture and Built Environment, University of Nottingham, Nottingham, UK*
[c] *University of York, York, UK*

ARTICLE INFO

ABSTRACT

Exposure to airborne fine particulate matter ($PM_{2.5}$) is linked to multiple negative health effects and indoor sources are important contributors to personal exposure. Cooking is a common indoor source, but reported emission rates have high variability. Methods to quantify uncertainty in $PM_{2.5}$ cooking emission rates are investigated so that they can be used in probabilistic exposure models to evaluate interventions. Controlled tests were conducted to measure emission rates from the toasting of bread because it is simple and repeatable. Two methods were compared: residential kitchen field tests and large chamber tests. The *theoretical peak* calculation method was used to determine emission rates from time-resolved $PM_{2.5}$ concentration measurements. The large chamber tests produced more consistent results than the residential field tests, with a coefficient of variance almost an order of magnitude lower due to the improved control of variables. Then, the emission rates were normally distributed with mean $0.23\,\mathrm{mg/min}$ and standard deviation $0.067\,\mathrm{mg/min}$. However, this distribution may be less representative of normal behaviour. The resulting dataset can be combined with other sources to represent housing stock exposures in probabilistic models, enabling the exploration of exposure uncertainties and interventions. More generally, key recommendations when measuring $PM_{2.5}$ emission rates include: high temporal resolution measurements; custom calibration factors; identifying periods for emissions, mixing, and decay; constant ventilation rates; quantifying mixing conditions; and ensuring high quality decay data.

1. Introduction

Buildings contain airborne contaminants that originate from indoor sources, such as emissions from occupant activities, building materials and furnishings, and from outdoor sources. Of these, airborne fine particles with a diameter of $\leq 2.5\,\mu m$, known as $PM_{2.5}$ [1], are shown to cause the greatest harm to health [2,3]. $PM_{2.5}$ is respirable, so bypasses the body's primary defences [4]. Exposure to elevated concentrations of $PM_{2.5}$ over extended periods is linked to chronic respiratory and cardiovascular diseases, and cancer [4]. Worldwide, people spend most of their time in their own houses [5–7], where indoor sources of $PM_{2.5}$ have been found to have a greater effect on indoor concentrations than those from ambient sources [8], and so emissions from indoor sources are thought to be an increasingly important source of personal $PM_{2.5}$ exposure.

Cooking is an activity conducted in the majority of homes, where the complete removal of contaminant sources is generally impossible and ventilation is the sole means of dilution. It has frequently been identified as an indoor source of $PM_{2.5}$ by *in-situ* measurements in

dwellings [9–13], and several known carcinogens have been identified as constituents of cooking emissions [14]. Cooking emissions and poor kitchen ventilation are associated with elevated risks of lung cancer, particularly in women [15], and cooking using traditional woks in kitchens without a cooker hood is associated with an increased risk of lung cancer for non-smoking Taiwanese women [16]. However, the cooking method and conditions are not exclusive to Taiwan or Asia. Furthermore, a risk assessment of inhalation exposures to trace elements when cooking in under-ventilated spaces estimates that carcinogenic and non-carcinogenic risks were higher than safe levels for most elements considered [17]. However, concern has been raised about relating health effects directly with the diameter of particles alone, since $PM_{2.5}$ is a complex mixture of particles with a range of characteristics including size, chemical composition, metal content, and water solubility [18].

O'Leary et al. [19] identify five main factors in $PM_{2.5}$ emissions when cooking. The first is the method of cooking, where the emission rate increases with the degree of ingredient browning. Maillard browning occurs when amino acids react with sugars to form new substances,

---

and increases with ingredient temperature until charring occurs, at around 180. Secondly, the use of oil increases the likelihood of $PM_{2.5}$ emissions and is generally a function of its smoke point. Thirdly, non-essential additives, such as seasonings, increase emissions of $PM_{2.5}$ and other contaminants when terpenoids are present. Fourthly, there is a positive correlation between the fat content of ingredients and $PM_{2.5}$ emissions. Water content is also found to impact the distribution of particle sizes. Finally, cooking equipment (food cooked in stainless steel pans have higher emission rates than the same food cooked in non-stick pans) and the type of heat sources (gas burners have higher emissions than electric hobs) both influence emission rates.

There are two main methods for investigating exposure to cooking contaminants in dwellings. The first is to measure their concentrations *in-situ* using static or portable personal measurement devices [11,20]. Alternatively, contaminant transport models can be used to simulate an indoor environment and predict temporal variations in concentrations over time [21–25]. Both methods have their advantages, but, large scale *in-situ* monitoring is invasive, and cost and time prohibitive. Models of housing stocks can be used to estimate exposures at the population scale, and to predict the impacts of interventions [24,25]. To understand uncertainty in predictions, the models are simulated probabilistically, and so a probability distribution function (PDF) is needed to describe the uncertainty in each input. This approach interrogates the entire probability space and so interactions between inputs and outputs can be explored using a global sensitivity analysis [21,24–26]. Sensitivity analyses show that model predictions are highly sensitive to the contaminant emission rate [21,25].

Empirical measurements, required for probabilistic modelling, show that cooking emission rates are highly variable, even for the same cooking methods and ingredients [24]. This is even true for simple and repeatable cooking methods, such as the toasting of bread. For example, He et al. [11] and Dacunto et al. [27] show that median emission rates for toasting can vary between 0.11–9.5 mg/min, respectively. However, reported sample sizes are often small. For example, Dacunto et al. measured emission rates from 14 different cooking methods where the largest number of repetitions was six. He et al. also measured emission rates from nine different heating and cooking methods where the largest number of repetitions was 25. There is no indication that this data adequately represents the uncertainty in the central estimate. Errors are not always reported. This makes it difficult to use the data to produce the PDF.

A range of methods have been used to measure $PM_{2.5}$ emission rates, which differ in their choice of location (highly controlled spaces, such as small scale test chambers, to uncontrolled environments, such as personal monitoring *in-situ*), in their abstraction, their ability to control errors, in the time required to obtain data, and in incurred costs.

Therefore, the aim of this study is to develop a method to measure uncertainty in $PM_{2.5}$ cooking emissions, so that the data can be used to model uncertainty in exposures. The toasting of bread is used to refine the method because it is a simple, cheap, and repeatable cooking source. Section 2 introduces existing methods of estimating emission rates, and Section 3 describes those we use to determine uncertainty in proposed for this study. Section 4 presents the results for the emission rates calculation and other modelling parameters, and Section 6 summarises the key findings and takeaways.

2. Theory: existing methods of measuring emission rates

Existing methods of measuring emission rates from domestic cooking can be divided into five categories, each of which has its own benefits and frequency in the literature. The methods are given in order of increasing abstraction and, approximately, in order of decreasing costs. They are summarised in Table 1.

The first is personal monitoring, which is generally rare. Olson et al. [28] used this method to determine so called *personal* emission rates

using measurements of $PM_{2.5}$ concentration made during four, seven-day monitoring periods by 37 participants. Concentration peaks from cooking were identified and cross-referenced with the participants' diaries, and the emission rate calculated using a mass balance approach that considered a house to be a single well-mixed space. For a total of 411 cooking events, the emission rates ranged between 0.6 mg/min and 1496 mg/min ($\mu = 36$ mg/min and $\sigma = 98$ mg/min). However, the authors make it clear that these personal emission rates are high due to the proximity of the sensor to the source. Additionally, the true emission rates are likely to be further overestimated by the assumption that the whole house is well-mixed. The cooking methods were recorded, but details of the ingredients and cooking method were not, reducing the utility of the data for use in modelling.

The second approach uses monitors located in places of interest, frequently in dwellings. He et al. [11] measured $PM_{2.5}$ mass concentrations over 48 hour periods in 15 houses in Brisbane, Australia. Elevated concentrations were linked to *events* using occupant diary entries, and catalogued into 21 activity types; 106 of 153 events were catagorised as cooking activities. Measurements of the air exchange rate (AER) and controlled cooking tests were conducted in each house. This provided an opportunity for a direct comparison between houses. Emission rates were determined using a mass balance relationship and ranged between 0.03–2.78 mg/min with a mean of $\mu = 0.11$ mg/min. The lack of control over ventilation rates and emission periods led to large errors. Nasir & Colbeck [29] followed the same method in English dwellings and estimated emission rates for oven grilling (1.70 ± 0.27 mg/min, $n = 10$), boiling (1.00 ± 0.21 mg/min, $n = 15$), and frying (1.47 ± 0.75 mg/min, $n = 10$). Chan et al. [20] developed an algorithm to identify emission periods and estimate emission rates from 224 days of monitoring in 18 California apartments. Their method did not require occupant activity diaries, but this means the source types are unknown. Overall, 836 distinct events were identified, with a geometric mean and standard deviation of $\mu = 0.67$ mg/min and $\sigma = 0.07$ mg/min, respectively. In a non-domestic study, See & Balasubramanian [30] monitored fine and ultrafine ($PM_{0.1}$) particles in a typical Chinese food stall in Singapore. Studies of commercial cooking are useful for understanding the nature of particle emissions from cooking. Conversely, concentrations and emission rates reported may be less applicable due to differences in cooking behaviour and duration, and quantities of food prepared.

The third method uses managed tests conducted in semi-controlled conditions in the field, typically in a residential setting; see Dacunto et al. and Fortmann et al. [27,31]. Both studies investigated emission rates from a variety of sources, and conducted some tests in a residential setting using gas and electric stoves. They used different mass balance relationships to estimate emission rates. The AERs were measured using tracer gas decay, and the test environments purged with outdoor air between tests. Dacunto et al. [27] conducted 66 measurements in three locations, including both cooking and non-cooking sources with duplicates of most, but not all, tests. The lowest emission rate of 0.1 mg/min was from oven cooking frozen pizza, whilst the highest cooking emission rate of 15.2 mg/min was from frying chicken breast. Fortmann et al. [31] conducted 32 cooking tests using a variety of foods and cooking methods based on the US diet, under multiple ventilation conditions, in a single location. Seven tests were repeated to compare changes using gas and electric heat sources, and four tests were duplicated exactly to investigate variability, the results of which suggested high variability that exceeded 100% and a need for more repetitions. Estimated emission rates ranged from 0.025 mg/min for roast pork with exhaust ventilation, to 10.3 mg/min when frying tortillas on an electric range. The range of emission rates from both of these studies highlights the need to understand the population diet when choosing food sources to investigate, whilst the low repeatability - indicated in the repeatability tests [31] and large standard deviations [27] - calls for more repetitions.

The fourth measurement method employs large scale chambers to obtain a further level of control over ventilation rates and mixing

Table 1

Summary of existing methods for measuring PM$_{2.5}$ emission rates. Methods are given in order of increasing abstraction and in order of approximate decreasing costs.

| Method	Description	Benefits	Drawbacks	Frequency in literature
Personal monitoring	Measure PM$_{2.5}$ concentrations during occupant activities using portable monitors	Directly captures real-world conditions	Invasive, biased by proximity to food and whole-house mixing assumption	Rare
In-situ monitoring	Measure PM$_{2.5}$ in homes and identify peaks from occupant activity diaries	Natural conditions, direct source identification	Less control over conditions, reliance on diaries. Biased by proximity to food, mixing assumption, differences in cooking behaviour, duration, and quantities of food prepared.	Frequent
Managed field tests	Controlled emission tests conducted in residential settings.	Some control of conditions, comparison between locations, occupant diaries not required.	Time-consuming, low repeatability	Occasional
Large chamber tests	Use large environmental chambers to control conditions	High control of mixing, ventilation, materials	Abstracted conditions	Occasional
Small chamber tests	Use small test chambers or fume hoods	Very controlled conditions	Highly abstracted conditions	Occasional
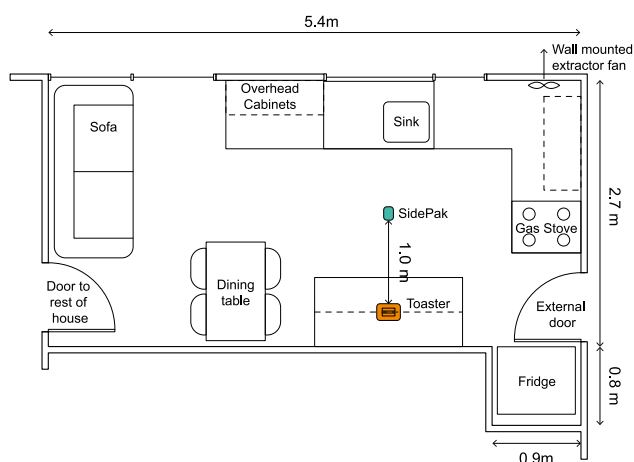
Fig. 1. Phase 1 residential kitchen with a volume of 35.4 m^3 and located in Nottingham, UK.

conditions, contaminant concentrations in the supply air, and internal materials to minimise sink effects. By creating a test chamber within a building, the effect of outdoor air and natural ventilation processes is reduced, and over-pressuring the test chamber controls the direction of background ventilation [32]. [32] investigated concentrations of fine and ultrafine particles from 10 cooking and non-cooking sources, under identical conditions, in a full-scale test chamber. Lee et al. [33] found PM$_{2.5}$ emission rates of 0.72–1.83 mg/min, for five mosquito coils tested in a large environmental chamber. Temperature, relative humidity, AER, mixing conditions and leakage were all controlled during these tests, which reduces error in the estimated emission rates. Finally, Pagels et al. [34] investigated the chemical composition and mass emission of candle smoke particles. Although these are not cooking sources, the method is of interest, because it used a positively pressurised stainless steel chamber, with controlled relative humidity, temperature, ventilation rates and mixing conditions, and filtered supply air [34].

The fifth and final method uses small scale chambers. Géhin et al. [35] utilised a hexagonal test chamber, volume 2.36 ± 0.05 m^3, first designed for vacuum cleaner efficiency characterisation, to investigate fine and ultrafine particle emission rates for cooking and non-cooking sources. The control measures used in large chamber tests were used plus an antistatic coating on internal surfaces and an upward current

of filtered air to reduce sink effects. Torkmahalleh et al. [36] measured emissions when heating cooking oils in a laboratory fume hood operating at 65 m^3/h (80 h^{-1}), with 5 repetitions of each test. Mixing conditions were tested using SF$_6$ as a tracer gas and a grid with points located 10 cm apart. The small space volume meant the air was very well mixed, but the method of heating the cooking oils in a beaker on a hot plate was far abstracted from real cooking methods, and so the resulting emissions may not reflect those found in a domestic kitchen. This may also be true for the emissions from Géhin et al. [35] where the forced airflow conditions could have impacted the emissions from the combustion source.

3. Methods

This study conducted two phases of tests, each using a different method. Phase 1 following the controlled field test method used by Dacunto et al. and Fortmann et al. [27,31]. Problems were encountered during Phase 1, described in Section 4, and so a second phase of tests was initiated. Phase 2 used conditions similar to found in field tests, described by Dacunto et al. [27], and combined them with large-scale chamber tests, described by Afshari et al. [32].

3.1. Phase 1: Controlled field tests

The first tests were conducted in a residential kitchen during the cooling season, with a volume of 35.4 m^3, located in Nottingham, UK; see Fig. 1. It was not possible to precisely control the ventilation rate. However, all windows and internal and external doors were closed during testing, and the installed wall-mounted kitchen extractor fan was used to depressurise the space and stabilise the ventilation rate. The ventilation rate was not measured and mixing conditions were not directly investigated.

A SidePak™ AM510 Personal Aerosol Monitor (SidePak) was used to monitor PM$_{2.5}$ concentrations, at height 1.1 m, 1 m from the source; see Fig. 1. The limitations of this optical device are discussed by Jones et al. [37]. Concentrations were time-averaged and reported at 1 min intervals following Ott et al. [38]. The default calibration factor (CF) of 1.0 was set as no concurrent gravimetric sampling was available; see Section 3.1.2.

The test consisted of toasting two slices of bread (medium sliced white or wholemeal Hovis 800 g loaf) in a supermarket branded 870 W toaster on its highest setting. The toaster was new at the start of testing and was not cleaned between tests. The test was chosen to be simple and repeatable; the toaster had a predefined cooking time (around

3 min) and temperature, and the bread slices were consistent in weight and geometry. The start and end times of the toasting period were recorded. The room was monitored under constant conditions for at least 25 min between tests to allow PM$_{2.5}$ concentrations to return to background levels. The test was repeated a total of 40 times, evenly split between white and wholemeal bread. The toast was cooked until the colour changed to dark brown, almost burnt in some cases.

To further investigate the concentration profile during the emission period, an additional six *plume tests* were conducted in the same location. During these tests, a sample tube attached to the SidePak inlet was positioned in the plume, 20 cm above the toaster, and concentrations were logged at 1 s intervals. Here, the decay period was not monitored and the room was flushed with outdoor air between tests. These were used to check that the toaster was the emission source of PM$_{2.5}$, that emissions were restricted to the emission period –also known as α–period– and to verify that the emission rate was constant; see Section 4.1.2.

3.1.1. Calculation of the rates of emission and decay

The method used to determine PM$_{2.5}$ emissions rates was based on the *theoretical peak* mass balance model following [27,28,38] and uses measurements of PM$_{2.5}$ concentration, $C(t)$ ($\mu g/m^3$), as a function of time, t (s). It is the most commonly applied method in the literature and assumes a constant emission rate during the emission or α–period, with duration $t = T$. The period of time after the source stops emitting and when the concentration decays is known as the γ–period. However, determining the mean emission rate solely using the α and γ periods assumes that the contaminant is instantaneously mixed in a space. Ott et al. [38] suggest that when the observed peak concentration occurs after the end of the α–period, a mixing period exists between the α and γ periods known as the β–period. Then, the emitted PM$_{2.5}$ is not yet fully mixed with room air, whereas during the γ–period the air is well mixed and smooth decay occurs. The end of the β–period and start of the γ–period is identified as the time within the decay period when the peak concentration occurred. Fig. 3 shows an example of the β and γ periods for one test. The total decay rate, ϕ (s^{-1}), is the sum of all removal mechanisms attributable to ventilation and other mechanisms. It is determined from the log-linear regression of the PM$_{2.5}$ concentrations during the γ–period. The estimated value of ϕ is then used to extrapolate the concentration back through the β–period to estimate the *theoretical peak* concentration, C_p ($\mu g/m^3$), the predicted concentration at the start of the β–period and end of the α–period; see Fig. 3. Then, the emission rate, g ($\mu g/s$) can be determined by

$$g = \phi V \left[\frac{C_p - C_b - (C(0) - C_b)e^{-\phi T}}{1 - e^{-\phi T}} \right] \tag{1}$$

where C_b is the background concentration ($\mu g/m^3$), $C(0)$ is the initial concentration ($\mu g/m^3$) when $t = 0$, and V is the mixing volume (m^3).

The measured concentrations were split into α–period and non-α–periods using the recorded cooking times. The decay period was then further split into the β– and γ–periods. Custom MATLAB [39] code[1] was used to process the data. Tests were excluded when: (i) $R^2 < 0.7$ for the log-linear regression of the decay concentrations; (ii) the emission rate was negative; or (iii) the emission rate could not be estimated, because they indicate a problem with the test data.

Outlying data points were tested using *Chauvenet's Criteria* [40], and removed accordingly. Additionally, the non-parametric Mann–Whitney or Wilcoxon's Rank-sum test (MW test) was used to test for a statistically significant difference in the emission rates for toasting wholemeal or white bread, as a visual inspection of the distributions of g appeared non-normal.
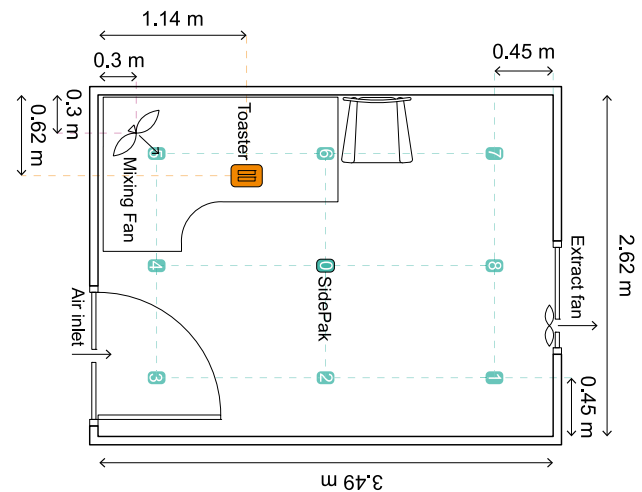
---

[1] The code is available under a creative commons license from DOI: 10.13140/RG.2.2.22824.32003

Fig. 2. Phase 2 outdoor test chamber with volume of 21.5 m^3 and located in Nottingham, UK.

3.1.2. Calibration factors

Gravimetric sampling can be used to determine an accurate mean average PM$_{2.5}$ concentration [41], which can be compared against that determined by a collocated photometer and used to calibrate it using a CF, a ratio of the two means [37]. Concurrent gravimetric sampling was not available, but Dacunto et al. [27] report CF = 0.47 for burned toast ($n = 3$) and Jiang et al. [42] measured CF = 0.79 ($n = 20$) for toasting bread. They also attributed the difference to levels of charring, referring to a *char index*. It was not possible to obtain details of this char index for comparison, so in the absence of further information, the data set was processed twice, applying each CF directly to the measured concentrations in turn.

3.2. Phase 2: Large-scale chamber tests

A second set of tests were conducted in an outdoor chamber, also during the cooling season, with a volume of 21.5 m^3, located in Nottingham, UK; see Fig. 2. Plastic sheeting was laid on the floor to minimise resuspension, and unnecessary furniture and fixings were removed. Custom boards were installed into the open window and door to control the ventilation conditions. A low level 0.1×0.1 m opening was located in the doorway, and an extractor fan (XF100S 15 W, Manrose, Reading, UK) with a target exhaust flow rate of 85 m^3/h (23 L/s) was fitted into the window. A small portable fan was used to aid mixing within the chamber and whose effects are considered in Section 5.

Two SidePaks measured PM$_{2.5}$ mass concentrations at 1 s intervals, increasing the resolution above the 1 min sampling frequency used for Phase 1. Both SidePaks were mounted on tripods at a height of 1.1 m. The first, named SidePak$_F$, was fixed at position 0 shown in Fig. 2, whereas the second, named SidePak$_R$, was rotated between all 9 positions between tests to investigate the chamber mixing conditions; see Section 3.2.1. Only the concentrations from SidePak$_F$ were used to calculate emission rates. SidePak$_R$ was used in investigate mixing conditions in Section 3.2.1.

In addition, two IAQ-Calc Indoor Air Quality Meters (Model 7545, TSI Inc., Shoreview, MN, USA) were used to monitor indoor and outdoor temperature, CO$_2$ concentration, and relative humidity. Chamber relative humidity was maintained below 70% throughout testing to reduce its influence on SidePak performance, and an electric oil-filled radiator was used to heat the chamber when required.

Both SidePaks measured background PM$_{2.5}$ concentrations for a 5 min period at the start of each test day to establish a value for C_b. The SidePaks were then moved indoors, the boards were fitted

to the window and doorway, and the extractor fan was turned on before commencing testing. The Phase 1 method was followed where each test consisted of toasting two slices of bread in the same toaster located on a table (see Fig. 2) for a total of 40 repeats. Unlike Phase 1, all tests were conducted using wholemeal bread (Hovis, medium slice 800 g) as no statistically significant difference in emissions between the toasting of white and wholemeal bread was observed during Phase 1; see Section 3.1.1. The start and end of the α–period were recorded when the toaster was switched on and when toasting ended. A box was placed over the toast and toaster at the end of the α–period to prevent further $PM_{2.5}$ emissions as the bread and toaster cooled. $PM_{2.5}$ concentrations were then monitored under steady conditions for a 20 min decay period. The room was then purged with outdoor air to return chamber $PM_{2.5}$ concentrations to C_b.

3.2.1. Mixing conditions

To check that the main sampling location provided a representative $PM_{2.5}$ concentration for the test chamber, the location of $SidePak_F$ was fixed for all tests, whereas the location of $SidePak_R$ was varied between tests. Both SidePaks were collocated during the first test of each test day. For each subsequent test, $SidePak_R$ was moved sequentially through Positions 0–8. Jiang et al. [42] reported some variation in CF between SidePaks. Therefore, when both SidePaks were in Position 0 (once every 9 tests), a relative CF (rCF) was calculated to adjust the concentrations reported by $SidePak_R$ until both were again collocated. The rCF was taken to equal the ratio of the mean concentrations measured by $SidePak_F$ and $SidePak_R$. The concentrations reported by both SidePaks were compiled and the overall distributions of concentrations were compared for each location using Q-Q plots and a Mann–Whitney test was used to check for statistical significance.

3.2.2. Calibration tests

Gravimetric sampling was unavailable during the early stages of the Phase 2 test period, and so the CF was initially set at 1.0. Later, a MiniVol Tactical Air Sampler (MiniVol) (Airmetrics, Eugene, OR, USA) was used to determine CFs. It drew air through a $PM_{2.5}$ impactor and a pre-weighed 47 mm Millipore Fluoropore™ PTFE membrane filter at rate of $q = 0.13$ l/s. To ensure there was detectable mass deposited on its filter, the $PM_{2.5}$ concentration was increased by reducing the chamber ventilation rate by closing the door and window for the duration of each test. The MiniVol was collocated with both SidePaks in the centre of the test chamber (Position 0, Fig. 2). Three calibration tests were conducted. Tests 1 and 3 consisted of 5 sequential repetitions of the toasting of two slices of bread (Hovis, wholemeal 800 g medium sliced), which was followed by a short decay period, whereas test 2 consisted of a single repetition of toasting 2 slices of bread followed by a long decay period of around 1.5 h. Tests 1 and 3 were designed to be high concentration tests, and Test 2 was a low concentration test. The start and end time were recorded for each filter. The toast and toaster were sealed in a container between α–periods as they were for the main Phase 2 tests. A single filter was used for each test and the chamber was flushed with outdoor air between tests.

Filters were pre and post weighed under controlled conditions to determine the total mass collected, m (μg) over a measurement duration, D (s). The average mass concentration, $\overline{C}$ (μg/m^3), was determined for each filter by

$$\overline{C} = \frac{m}{qD} \tag{2}$$

Mean SidePak concentrations were calculated over the duration of the measurement period, D. Calibration factors were determined separately for each SidePak using regression analysis with the intercept forced through the origin. In addition, a combined calibration factor for both SidePaks was determined using linear regression. All CFs were determined using Microsoft Office Excel 2013.
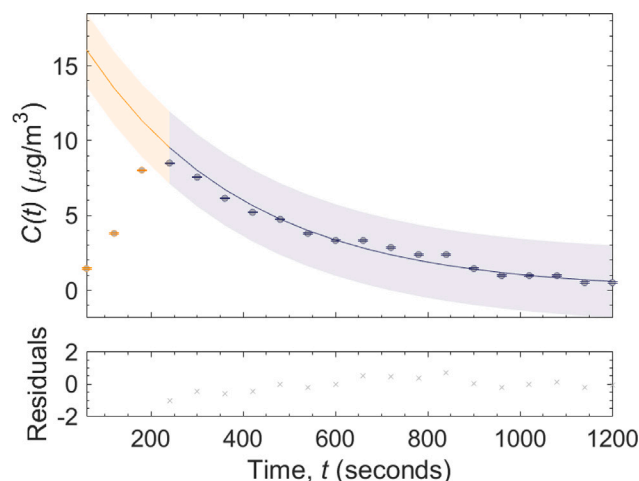

Fig. 3. Example concentrations over time during the decay period following one of the tests. Orange, β-period; Blue, γ-period. (For interpretation of the references to colour in this figure legend, the reader is referred to the web version of this article.)

3.2.3. Data analysis

The data was analysed using custom MATLAB[2] code. This code is an update of that used in Phase 1 to estimate emission rates, and accommodates an increase in noise that occurs as a consequence of the increase in sampling frequency to 1 s.

To calculate the emission rate, the combined CF (see Section 3.2.2) was first applied to the measured $PM_{2.5}$ concentrations. Then, the data was isolated for each test in turn, and the α–period was removed based on recorded test times, T. In Phase 1, the end of the β–period was identified by the peak concentration. In this phase, the updated MATLAB code searched for the smooth decay period (β and γ) using log-linear regression and the coefficient of determination (R^2) as a test for the goodness of fit. The regression was conducted iteratively for the entire decay period by removing one point at a time at the beginning of the decay period and recording the R^2. This iterative process was carried out for the first 25% of decay period data points. The retained data set was recorded as the γ–period, its starting time was set to zero, and C_b was subtracted from each concentration measurement. All subsequent stages of the analysis followed the Phase 1 method, where the decay rate was extrapolated back through the β–period to predict C_p, and the emission rate was calculated using Eq. (1).

The calculated decay rates were summarised for comparison against the expected ventilation rate of the installed fan. Finally, the emission rates were used to produce an empirical cumulative distribution function whose shape was investigated to see if it could be approximated by a recognised distribution.

4. Results

4.1. Phase 1: Controlled field test

4.1.1. Emission rates calculation and calibration factors

Fig. 3 shows the concentrations over time during the decay period for a sample test with the fitted decay curve. The β–period is highlighted in orange and the γ–period is in blue. 30 of the original 40 tests met the acceptability criteria defined in Section 4.4.

Table 2 gives emission rates determined using CF = 0.47 and CF = 0.79. The distributions are similar for both CFs, and have a significant positive skew, where the median is much smaller than the mean. This is attributed to a few tests with a high emission rate. Table 2 also shows the substantial impact the CF has on the emission rate.

Table 2
Phase 1 emission rates, g (mg/min), $n = 30$.

	CF = 0.47			CF = 0.79		
	All	Wholemeal	White	All	Wholemeal	White
Min	0.003	0.003	0.02	0.02	0.02	0.03
LQ	0.04	0.03	0.04	0.06	0.05	0.06
Median	0.06	0.06	0.07	0.10	0.09	0.11
UQ	0.20	0.12	0.20	0.33	0.21	0.33
Max	22	22	0.47	37	37	0.78
Mean	0.9	1.7	0.13	1.6	2.9	0.22
SD	3.9	5.6	0.13	6.6	9.4	0.23
GM	0.09	0.09	0.08	0.16	0.17	0.14
GSD	5.5	9.1	2.8	5.1	7.9	2.8
N	30	15	15	37	15	15

LQ, lower quartile; UQ, upper quartile; SD, standard deviation;
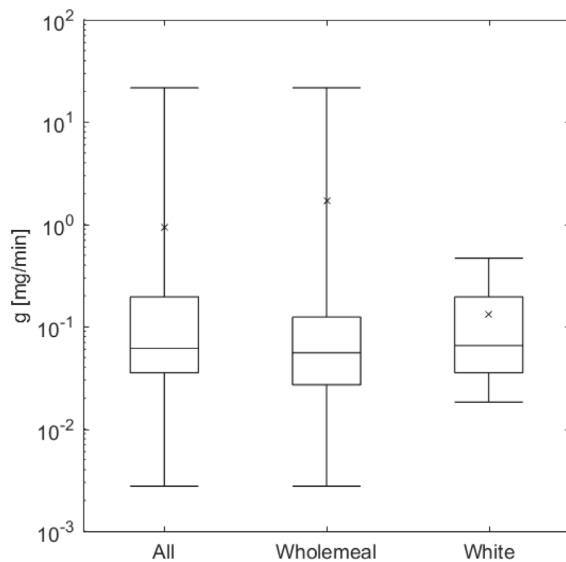GM, geometric mean; GSD, geometric standard deviation.

Fig. 4. Phase 1 emission rates distribution comparison CF = 0.47. Whiskers indicate the minimum and maximum emission rates. All: $N = 30$; Wholemeal: $N = 15$; White $N = 15$.

Fig. 4 shows the distribution of emission rates for *all* tests, *wholemeal* bread tests, and *white* bread tests when CF = 0.47. A MW test indicates the white bread and wholemeal bread emission rates were not significantly different at the $p < 0.05$ significance level.

4.1.2. Plume tests

Fig. 3 shows that the peak concentration in the initial tests occurred after the end of the α–period. The reasons for this were unclear, and the 1 min resolution of the recorded data made it difficult to conduct further investigations, especially as the toasting time was only around 3 min. The theoretical peak calculation method assumes this lag is due to the time taken for the $PM_{2.5}$ to fully mix within the space. However, emissions may have continued after toasting ended as the toast and toaster were not sealed at the end of the α–period. Alternatively, the particle composition and chemistry may have changed over time. The plume tests were used to investigate these areas of uncertainty.

Fig. 5 shows the plume test measurements of $PM_{2.5}$ during the α–period of all 7 tests. It confirms that $PM_{2.5}$ were emitted during toasting, and indicates that the emission rates, indicated by the gradients of the concentrations over time, are not constant throughout the α–period. However, the peak concentration did occur at the end of the α–period, and so the peak estimation method might still provide a reasonable estimation of g.
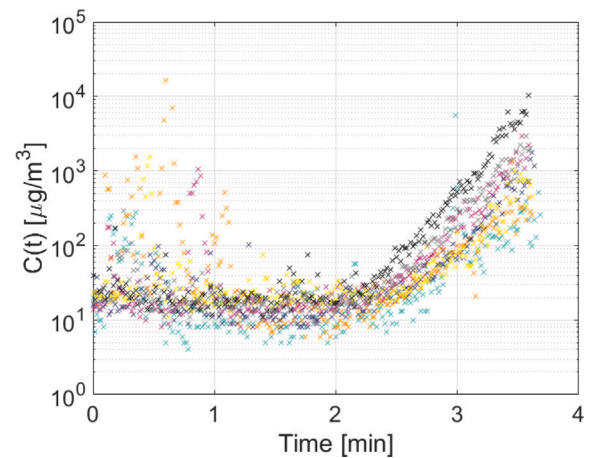

Fig. 5. Plume test concentrations demonstrating variable emission rate during the α–period of all 7 tests (CF = 1.0), $N = 7$.

Table 3
Calibration factors.

	CF	R^2	SE
SidePak$_F$	0.68	0.999	0.017
SidePak$_R$	0.59	0.999	0.015
Combined	0.63	0.997	0.022

4.2. Phase 2: Large-scale chamber tests

4.2.1. Mixing conditions

The relative CFs (rCFs) described in Section 3.2.1 were used to correct the SidePak$_R$ concentrations to match those from SidePak$_F$ ranged between 0.82 and 0.94 with $\mu = 0.89 \pm 0.04$. With the rCFs applied, the MW test found a statistically significant difference between SidePak$_F$ and SidePak$_R$ in Positions $2-8$ but not in Position 1, nor when they were collocated in Position 0. However, the statistical significance tests do not fully describe the mixing conditions in the chamber.

A comparison of quantiles for each device at each location shows good agreement between both SidePaks at lower concentrations. At higher concentrations, SidePak$_F$ measured higher concentrations than SidePak$_R$. A possible explanation for this difference was found by comparing time-resolved $PM_{2.5}$ concentrations during a sample test in each location where SidePak$_F$ appears more sensitive to the concentration increase due to toasting, but both SidePaks showed good agreement during the decay period. There was also a similar, smaller discrepancy when the SidePaks were collocated. The reason for this discrepancy is unclear, but may relate to noise in the data.

Overall, these tests indicate good mixing in the smooth decay period but not before. The time taken to achieve good mixing was accounted for by theoretical peak calculation method by using the γ–period data to estimate the theoretical peak.

4.2.2. Calibration factor

Fig. 6 shows a plot regressing the average concentrations from the gravimetric sampling against the average concentrations measured by each SidePak both separately and combined. The resulting CFs, R^2 and standard errors (SE) are reported in Table 3. The high R^2 values indicate the linear regression model is a good fit, even for the combined regression, which has a higher associated standard error.

4.3. Decay rates

The decay rates ranged between $0.09\,\text{s}^{-1}$ and $0.38\,\text{s}^{-1}$ with $\mu = 0.23 \pm 0.07\,\text{s}^{-1}$. All the predicted decay rates were larger than the
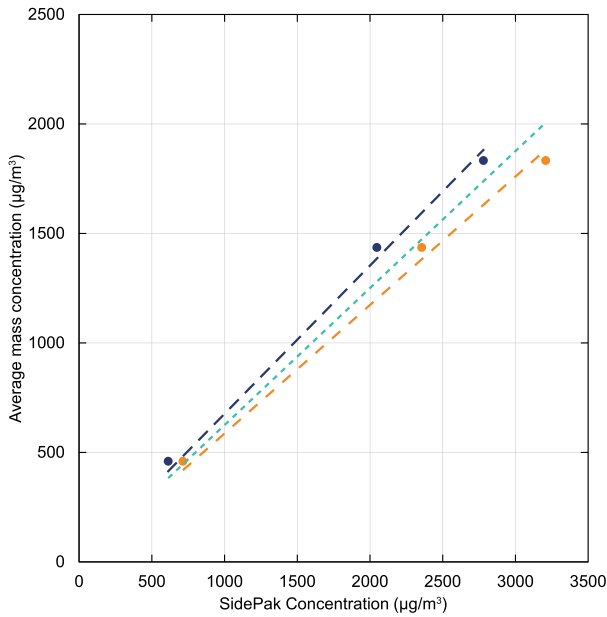
Fig. 6. Calibration factor (CF) test regressions. blue: $SidePak_F$ CF = 0.68; orange: $SidePak_R$ CF = 0.59; teal: Combined CF = 0.63. (For interpretation of the references to colour in this figure legend, the reader is referred to the web version of this article.)

Fig. 7. Example test decay concentrations, fitted decay curve, and residuals for wholemeal bread. CF = 0.63. Orange: β–period; blue: γ–period. (For interpretation of the references to colour in this figure legend, the reader is referred to the web version of this article.)

4.4. Emission rates

Fig. 7 shows the concentrations over time for a sample test and the corresponding decay concentrations with the fitted decay curve. As before, the α–, β– and γ–periods are distinguished by colour. The noisy data that necessitated the updated method to identify the γ–period is evident in Fig. 7. Three of the original 40 tests were rejected due to an $R^2 < 0.7$ and all the remaining tests produced positive emission rates. In addition, no tests were rejected by *Chauvenet's Criteria*, so $n = 37$.

Table 4
Phase 2 emission rates (mg/min).

CF	Min	LQ	Median	UQ	Max	μ	σ	CV	n
0.63	0.09	0.18	0.22	0.27	0.38	0.23	0.067	0.30	37

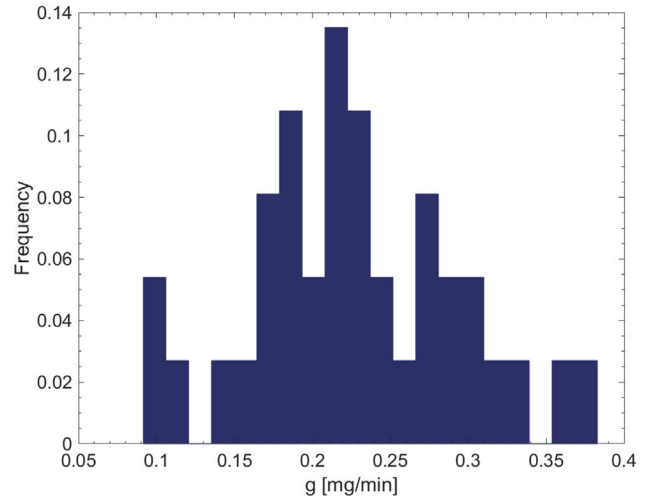
Fig. 8. Histogram of emission ratesfrom wholemeal toast. median = 0.22, μ = 0.23, σ = 0.067, N = 37.
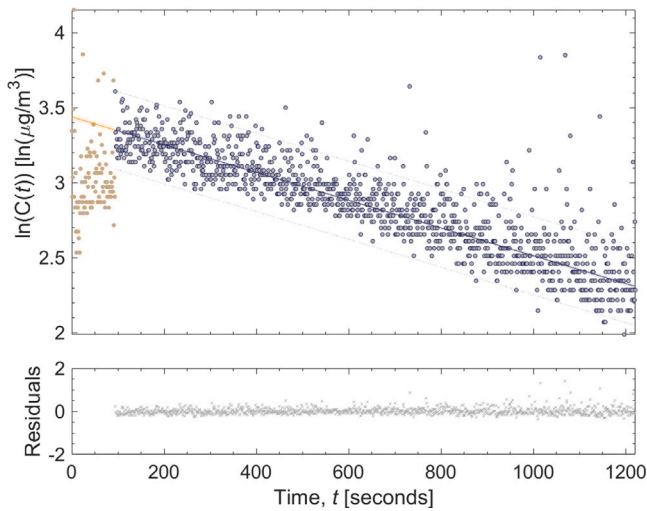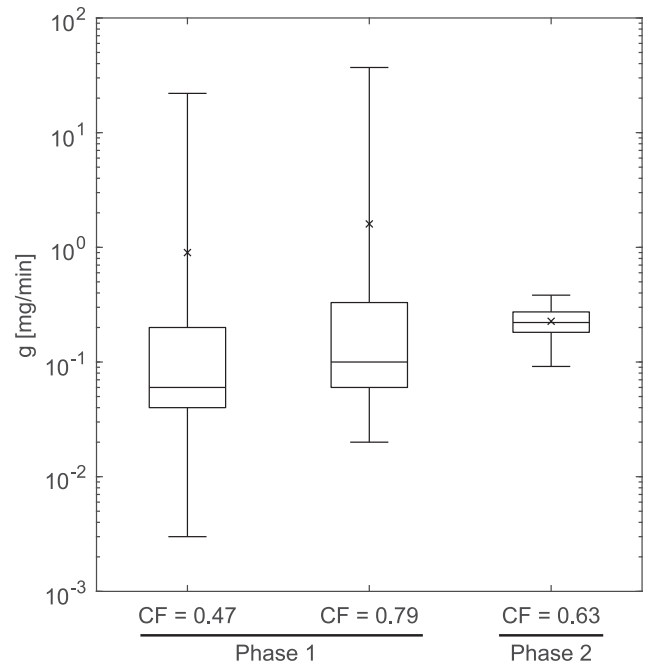

Fig. 9. $PM_{2.5}$ emission rate from the toasting of bread. A comparison between Phase 1 ($N = 30$ for each CR) and Phase 2 ($N = 37$). Descriptive statistics are in Table 5..

Unlike in Phase 1, the emission rates were close to normally distributed, which is to be expected as a distribution of mean values should follow the central limit theorem and is, therefore, reassuring. The tests produced consistent emission rates, and the mean and median were almost equal, see Table 4 and Fig. 8. Fig. 9 also includes a direct comparison to the results from Phase 1. The mean g was lower in Phase 2 when compared to the Phase 1 g with either CF, however the Phase 2 median g was higher. This plot also highlights that the Phase 2 g distribution was considerably less spread; the lower variance indicates the Phase 2 test method resulted in more consistent emission rates.

estimated air change rate of $0.001\,\text{s}^{-1}$. This indicated that deposition or other factors may have contributed more to the decay rate than ventilation. However, the decay still appeared first order logarithmic (see Fig. 7) and close to normally distributed.
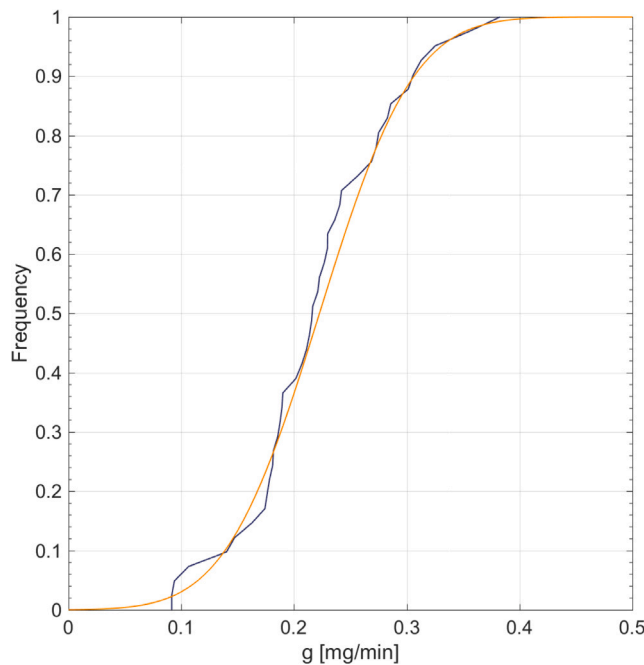
Fig. 10. Uncertainty in PM$_{2.5}$ emission rates from toasting bread during Phase 2. Blue: empirical CDF; Orange: normal CDF.. (For interpretation of the references to colour in this figure legend, the reader is referred to the web version of this article.)

Finally, an empirical cumulative distribution function (eCDF) was produced from the predicted emission rates, see Fig. 10. This eCDF could itself be used as an input for probabilistic modelling. Alternatively, a normally distributed cumulative distribution function (CDF) with $\mu = 0.23 \pm 0.067$ could also be used. This CDF is overlaid in orange in Fig. 10 and appears to be a reasonably good approximation of the eCDF.

5. Discussion

The mean emission rates from both Phase 1 and 2 were an order of magnitude lower than those reported by Dacunto et al. and Jiang et al. [27,42], see Table 5. The degree of charring might explain this difference. Dacunto et al. and Jiang et al. used a standard char-index to report the degree of charring in their tests, however it was not possible to obtain this index for comparison. The estimated mean emission rate for Phase 2 is closer in magnitude to the median 0.11 mg/min reported by He et al. [11].

Other than the changes in the measurement method, a possible further reason for the difference in emission rates between Phase 2 and Phase 1 is the characteristics of the bread itself. The same brand of wholemeal bread was purchased in Phase 1 and Phase 2, however, the manufacturer appeared to have adjusted the properties of the loaf in this time. In Phase 1, the slices of bread were rectangular and the top portion did not fit into the toaster, whereas in Phase 2, they were nearly square and most of the slice was toasted. This change may not itself have influenced g, but may also be indicative of other changes to the bread which could have a confounding effect. This variation could have been corrected if the slices had been weighed and measured before each test.

In Phase 1, the variance of the emission rates, indicated by the coefficient of variance (CV), remained large despite the high number of repetitions compared to the previous studies. The test method from Phase 1 was not highly repeatable and so the improved method in Phase 2 used a smaller room volume with improved mixing to give more resolution in the α–period. This resulted in a more reproducible test indicated by an CV that was an order of magnitude lower than in

Table 5
Emission rates comparison (mg/min).

	μ	σ	CV	N
Phase 1 CF = 0.47	0.9	3.9	4.33	30
Phase 1 CF = 0.79	1.6	6.6	4.13	30
Phase 2 CF = 0.63	0.23	0.07	0.30	37
Toast, 90–95% char [27]	9.5	10.8	1.14	3
Toast, 70–80% char [42]	4.2			
Toasting, [11]	0.11[a]	0.37	3.36	18

[a] Median.

Phase 1. The γ–period decay rates were also consistent in Phase 2 and fewer tests were rejected due to a poor model fit.

In Phase 1 the emission rates were not normally distributed, and the histograms suggest a distribution closer to log-normal. The main cause of the skew was a single test with high emission rates. No details were recorded in the test log that might indicate a reason for higher emissions during this test. The more consistent results in Phase 2 might be an indication of a more consistent test method, but the resulting distribution may be less representative of emissions under normal conditions. He et al. [11] determined emission rates from residential monitoring data. Their approach results in greater uncertainty derived from: (i) differences between toasting events, (ii) a dependence on occupant records of cooking events, and (iii) less control over the ventilation conditions.

However, He et al. [11] determined g from monitoring normal occupant behaviour, and so their distribution of g might be more representative of those experienced in a housing stock if the authors used representative sampling techniques to select participating households.

In Phase 1, the calibration factor was the largest source of uncertainty because gravimetric sampling was not used. During Phase 2, this source of uncertainty was reduced by conducting follow up gravimetric sampling to determine a custom CF. However, this method was not perfect, as the gravimetric sampling was not concurrent. The CFs of 0.59, 0.68, and 0.63 determined in Section 4.2.2 are all comparable to the CF = 0.79 from Jiang et al. [42] and CF = 0.47 from Dacunto et al. [27] for toasting bread. Jiang et al. also found SidePak CFs varied between devices, therefore there is precedent for the differing CFs for the two SidePaks used here. Although the use of combined CF is a source of additional error, it was selected over the SidePak$_F$ CF (fixed position) to accommodate additional uncertainty, as the CFs were not determined during the original test period and were based on just three filter samples.

In multiple tests during Phase 2, a high peak PM$_{2.5}$ occurred at the end of the α–period. These concentrations frequently dropped off rapidly at the start of the β–period. It is possible that the high peaks were due to the room air initially being poorly mixed. The mixing condition results also suggest that this may be the case, as a comparison of comparing time-resolved concentrations indicates that these high measured peaks were only measured for Point 0 at the centre of the chamber. The predicted C_p (see Eq. (1)) intercepts from the γ regression were typically lower than these high measured peak concentrations, indicating the method to identify the smooth decay period effectively ignored this initial drop-off. If mixing was the only cause, then this identifies a potential strength of the method. However, an alternative explanation for this initial rapid decay might be that some of the emitted PM$_{2.5}$ dissipated rapidly due to second-order decay mechanisms which were not constant over time. If this were the case, then the current method might have underestimated C_p and hence underestimated g. Nevertheless, the initial rapid decay would also then indicate these particles would not remain in the air for long, and so the risk of them being inhaled is lower.

The theoretical peak estimation method may also be a source of uncertainty as this method assumes a constant emission rate, g, over the α–period. The plume tests indicated that g was not constant over

time, with no $PM_{2.5}$ emissions in the first 2 min of the toasting period. After this time, the emission rate appeared to increase over time. This emission profile is expected for toasting, which relies on radiant heat transfer to first dry out and then brown the bread. As the toast browns, the rate of heat transfer also increases. One alternative approach to estimate emission rates was suggested by Pagels et al. [34], who determined the g iteratively by fitting a curve to the observed data and adjusting the emission rate to achieve the best possible fit. There are two potential problems with this alternative approach: firstly, Pagels et al. [34] still assumed a constant g over the α–period, and secondly, the predicted curve was based on the mass balance method which assumes instantaneous full mixing [38]. Neither was true here, therefore this method would not improve the peak estimation method.

A third option would be to use the area-under-the-curve method proposed by Ott et al. [38] to estimate the average emission rate $\overline{g(t)}$ over the α–period. This approach is theoretically exact, but it assumes instantaneous full-mixing, which was not observed in this case. In addition, the highest concentrations were observed at the end of the α–period, which was relatively short, therefore, the theoretical peak estimation method used here appears to be the most appropriate. This method is also best suited to accommodate the non-instantaneous mixing observed in Section 4.2.1.

One improvement of the method from Phase 1 to Phase 2 was that the mixing conditions within the chamber were investigated, and a desk fan was used to attempt to aid mixing. The results of these tests indicated good mixing within the chamber during the smooth γ–period. However, the mixing conditions were only investigated in two dimensions, that is, at the same height. Torkmahalleh et al. [36] measured the mixing conditions within their small test volume using SF_6 tracer gas and an array of sensors at 10 cm intervals. This method would better assess the mixing conditions throughout the chamber volume. The necessary equipment was not available within this study. In addition, if mixing conditions within the chamber were to be tested in future, it would be best to test the chamber both with and without a mixing fan, to determine whether it is necessary and the best position for it to be located. The behaviour of the researcher moving around the chamber operating equipment effects mixing randomly.

A key limitation of this test methodology is that it is time-consuming. Each phase of testing took 3 full days despite a short duration cooking activity of 3.85 ± 0.9 min.

Finally, toasting bread only represents a single cooking source, and so this data should be combined with other data to better represent the different cooking methods and ingredients used. The methods can be applied to other cooking approaches where any of the five main factors that affect $PM_{2.5}$ emission rates when cooking, which are introduced in Section 1. The data presented herein has already been used to estimate the exposure to cooking in Chilean houses and to determine the appropriateness of UK kitchen ventilation rates [24,25]. Cooking behaviour is variable and often includes activities of longer duration, thus, using these methods to measure emission rates from a range of sources would be very time-consuming. The Phase 2 method produced consistent emission rates, which suggested a normal distribution. If this can be replicated for other cooking sources, it might be possible to estimate cumulative distributions suitable for modelling assuming a normal distribution with a mean and standard deviation determined from a smaller sample size of tests.

Through this process, some important considerations for measuring g were identified: (i) the sampling frequency of optical devices should be as short as possible to maximise the quantity of data available for analysis; (ii) the need for concurrent gravimetric sampling to determine custom calibration factors used by an optical measurement devices used to measure temporal concentrations; (iii) the choice of an appropriate calculation method based on the shape of the emission source function; (iv) the need to identify the α, β, and γ periods used to determine emission and decay rates; (v) the ventilation rate itself does not need to be known, but the model does depend on a constant decay rate, and so

it must be steady; (vi) the need to measure and control chamber mixing conditions to ensure the decay rate is constant; and (vii) the quality of the concentration decay data.

6. Conclusions

Two phases of $PM_{2.5}$ emission tests were undertaken in different indoor environments; field tests in a residential kitchen, and large-scale chambers. Measurements made in a chamber produced more consistent results than those measured by field tests, with a coefficient of variance around an order of magnitude lower. This indicates that the improved control of variables increases repeatability. The *theoretical peak* calculation method was the most appropriate for these measurements because it accounts for the non-instantaneous mixing observed. However, it assumes a constant emission rate over the toasting period, which was not observed because the emission rate increased exponentially with time. The methods investigated are time intensive, so future work should investigate if normal distributions can be assumed for other sources based on small samples.

There are several key considerations that should be considered when measuring $PM_{2.5}$ emission rates from cooking: the use of high resolution temporal concentration data; concurrent gravimetric sampling for custom calibration; identifying the emission, mixing, and decay periods used to determine emission and decay rates; the ventilation rate does not need to be known but the removal rate should be steady; ensuring well-mixed conditions; and ensuring the high quality of the concentration decay data.

Finally, $PM_{2.5}$ emission rates for the toasting of bread are normally distributed with mean 0.23 mg/min and standard deviation 0.067 mg/min. This data can be use to probabilistically model exposures and evaluate interventions. This mean emission rate is lower than those reported by other studies and may be a function of the differences in a number of factors including the level of charring, which was not characterised here. The data is exclusively for the toasting of bread, and so it should be combined with measurements of other cooking sources to better represent real housing stock exposures.

CRediT authorship contribution statement

Constanza Molina: Writing – review & editing, Writing – original draft, Methodology, Investigation. **Benjamin Jones:** Writing – review & editing, Writing – original draft, Supervision, Methodology, Investigation. **Catherine O'Leary:** Writing – original draft, Visualization, Methodology, Investigation, Formal analysis, Data curation, Conceptualization.

Declaration of competing interest

The authors declare that they have no known competing financial interests or personal relationships that could have appeared to influence the work reported in this paper.

Data availability

Data will be made available on request.

Acknowledgements

References

[1] C.A. Pope, D.W. Dockery, Health effects of fine particulate air pollution: Lines that connect, J. Air Waste Manag. Assoc. 56 (6) (2006) 709–742, http://dx.doi.org/10.1080/10473289.2006.10464485.

[2] J.M. Logue, P.N. Price, M.H. Sherman, B.C. Singer, A method to estimate the chronic health impact of air pollutants in U.S. residences, Environ. Health Perspect. 120 (2) (2011) 216–222, http://dx.doi.org/10.1289/ehp.1104035.

[3] G. Morantes, B. Jones, C. Molina, M. Sherman, Harm from residential indoor air contaminants, Environ. Sci. Technol. (2023) In-review, TBD.

[4] J. Lewtas, Air pollution combustion emissions: Characterization of causative agents and mechanisms associated with cancer, reproductive, and cardiovascular effects, Mutat. Res./Rev. Mutat. Res. 636 (1–3) (2007) 95–133, http://dx.doi.org/10.1016/j.mrrev.2007.08.003.

[5] D. Lader, S. Short, J. Gershuny, The Time Use Survey, 2005: How We Spend Our Time, Report, Office for National Statistics, 2006.

[6] D. Lader, S. Short, J. Gershuny, The Time Use Survey, 2005: How We Spend Our Time, Report, Office for National Statistics, 2006.

[7] N.E. Klepeis, W.C. Nelson, W.R. Ott, J.P. Robinson, A.M. Tsang, P. Switzer, J.V. Behar, S.C. Hern, W.H. Engelmann, The national human activity pattern survey (NHAPS): A resource for assessing exposure to environmental pollutants, J. Exposure Sci. Environ. Epidemiol. 11 (3) (2001) 231.

[8] L. Morawska, A. Afshari, G.N. Bae, G. Buonanno, C.Y.H. Chao, O. Hänninen, W. Hofmann, C. Isaxon, E.R. Jayaratne, P. Pasanen, T. Salthammer, M. Waring, A. Wierzbicka, Indoor aerosols: from personal exposure to risk assessment, Indoor Air 23 (6) (2013) 462–487, http://dx.doi.org/10.1111/ina.12044.

[9] H. Ozkaynak, J. Xue, J. Spengler, L. Wallace, E. Pellizzari, P. Jenkins, Personal exposure to airborne particles and metals: results from the particle TEAM study in Riverside, California, J. Exposure Anal. Environ. Epidemiol. 6 (1) (1996) 57–78.

[10] E. Abt, H.H. Suh, G. Allen, P. Koutrakis, Characterization of indoor particle sources: A study conducted in the metropolitan Boston area, Environ. Health Perspect. 108 (1) (2000) 35–44.

[11] C. He, L. Morawska, J. Hitchins, D. Gilbert, Contribution from indoor sources to particle number and mass concentrations in residential houses, Atmos. Environ. 38 (21) (2004) 3405–3415, http://dx.doi.org/10.1016/j.atmosenv.2004.03.027.

[12] B. Brunekreef, N.A. Janssen, J.J. de Hartog, K. Meliefste, G. Hoek, T. Lanki, K.L. Timonen, M. Vallius, J. Pekkanen, R. Van Grieken, Personal, indoor, and outdoor exposures to $PM_{2.5}$ and its components for groups of cardiovascular patients in Amsterdam and Helsinki, Res. Rep. Health Eff. Inst. 127 (2005) 1–70, discussion 71–9.

[13] Y. de Kluizenaar, E. Kuijpers, I. Eekhout, M. Voogt, R.C.H. Vermeulen, G. Hoek, R.P. Sterkenburg, F.H. Pierik, J.H. Duyzer, E.W. Meijer, A. Pronk, Personal exposure to UFP in different micro-environments and time of day, Build. Environ. 122 (2017) 237–246, http://dx.doi.org/10.1016/j.buildenv.2017.06.022, URL http://www.sciencedirect.com/science/article/pii/S0360132317302561.

[14] K.L. Abdullahi, J.M. Delgado-Saborit, R.M. Harrison, Emissions and indoor concentrations of particulate matter and its specific chemical components from cooking: A review, Atmos. Environ. 71 (2013) 260–294, http://dx.doi.org/10.1016/j.atmosenv.2013.01.061, URL http://www.sciencedirect.com/science/article/pii/S1352231013000861.

[15] P.-L. Jia, C. Zhang, J.-J. Yu, C. Xu, L. Tang, X. Sun, The risk of lung cancer among cooking adults: A meta-analysis of 23 observational studies, J. Cancer Res. Clin. Oncol. 144 (2) (2018) 229–240, http://dx.doi.org/10.1007/s00432-017-2547-7.

[16] Y.C. Ko, C.H. Lee, M.J. Chen, C.C. Huang, W.Y. Chang, H.J. Lin, H.Z. Wang, P.Y. Chang, Risk factors for primary lung cancer among non-smoking women in Taiwan, Int. J. Epidemiol. 26 (1) (1997) 24–31, http://dx.doi.org/10.1093/ije/26.1.24.

[17] S. Gorjinezhad, A. Kerimray, M. Amouei Torkmahalleh, M. Keleş, F. Ozturk, P.K. Hopke, Quantifying trace elements in the emitted particulate matter during cooking and health risk assessment, Environ. Sci. Pollut. Res. 24 (10) (2017) 9515–9529, http://dx.doi.org/10.1007/s11356-017-8618-0.

[18] L.C. Green, E.A.C. Crouch, M.R. Ames, T.L. Lash, What's wrong with the national ambient air quality standard (NAAQS) for fine particulate matter ($PM_{2.5}$)? Regul. Toxicol. Pharmacol. 35 (3) (2002) 327–337, http://dx.doi.org/10.1006/rtph.2002.1548.

[19] C. O'Leary, Y. de Kluizenaar, P. Jacobs, W. Borsboom, I. Hall, B. Jones, Investigating measurements of fine particle ($PM_{2.5}$) emissions from the cooking of meals and mitigating exposure using a cooker hood, Indoor Air 29 (3) (2019) 423–438, http://dx.doi.org/10.1111/ina.12542.

[20] W.R. Chan, J.M. Logue, X. Wu, N.E. Klepeis, W.J. Fisk, F. Noris, B.C. Singer, Quantifying fine particle emission events from time-resolved measurements: Method description and application to 18 california low-income apartments, Indoor Air 28 (1) (2018) 89–101, http://dx.doi.org/10.1111/ina.12425.

[21] P. Das, C. Shrubsole, B. Jones, I. Hamilton, Z. Chalabi, M. Davies, A. Mavrogianni, J. Taylor, Using probabilistic sampling-based sensitivity analyses for indoor air quality modelling, Build. Environ. 78 (2014) 171–182, http://dx.doi.org/10.1016/j.buildenv.2014.04.017.

[22] J.M. Logue, N.E. Klepeis, A.B. Lobscheid, B.C. Singer, Pollutant exposures from natural gas cooking burners: A simulation-based assessment for Southern California, Environ. Health Perspect. 122 (1) (2014) 43–50, http://dx.doi.org/10.1289/ehp.1306673.

[23] C. Shrubsole, J. Taylor, P. Das, I.G. Hamilton, E. Oikonomou, M. Davies, Impacts of energy efficiency retrofitting measures on indoor $PM_{2.5}$ concentrations across different income groups in England: A modelling study, Adv. Build. Energy Res. (2015) 1–15, http://dx.doi.org/10.1080/17512549.2015.1014844.

[24] C. O'Leary, B. Jones, S. Dimitroulopoulou, I.P. Hall, Setting the standard: The acceptability of kitchen ventilation for the english housing stock, Build. Environ. (2019) 106417, http://dx.doi.org/10.1016/j.buildenv.2019.106417.

[25] C. Molina, B. Jones, I.P. Hall, M.H. Sherman, CHAARM: A model to predict uncertainties in indoor pollutant concentrations, ventilation and infiltration rates, and associated energy demand in Chilean houses, Energy Build. (2021) 110539, http://dx.doi.org/10.1016/j.enbuild.2020.110539, URL http://www.sciencedirect.com/science/article/pii/S0378778820314195.

[26] B. Jones, P. Das, Z. Chalabi, M. Davies, I. Hamilton, R. Lowe, A. Mavrogianni, D. Robinson, J. Taylor, Assessing uncertainty in housing stock infiltration rates and associated heat loss: English and UK case studies, Build. Environ. 92 (2015) 644–656, http://dx.doi.org/10.1016/j.buildenv.2015.05.033.

[27] P.J. Dacunto, K.-C. Cheng, V. Acevedo-Bolton, R.-T. Jiang, N.E. Klepeis, J.L. Repace, W.R. Ott, L.M. Hildemann, Real-time particle monitor calibration factors and $PM_{2.5}$ emission factors for multiple indoor sources, Environ. Sci.: Process. Impacts 15 (8) (2013) 1511–1519, http://dx.doi.org/10.1039/C3EM00209H.

[28] D.A. Olson, J.M. Burke, Distributions of $PM_{2.5}$ source strengths for cooking from the research triangle park particulate matter panel study, Environ. Sci. Technol. 40 (1) (2006) 163–169, http://dx.doi.org/10.1021/es050359t.

[29] Z.A. Nasir, I. Colbeck, Particulate pollution in different housing types in a UK suburban location, Sci. Total Environ. 445–446 (2013) 165–176, http://dx.doi.org/10.1016/j.scitotenv.2012.12.042.

[30] S.W. See, R. Balasubramanian, Risk assessment of exposure to indoor aerosols associated with Chinese cooking, Environ. Res. 102 (2) (2006) 197–204, http://dx.doi.org/10.1016/j.envres.2005.12.013.

[31] R. Fortmann, P. Kariher, R. Clayton, Indoor air quality: residential cooking exposures, Report, State of California Air Resources Board, 2001, URL http://www.arb.ca.gov/research/indoor/cooking/cooking.htm.

[32] A. Afshari, U. Matson, L.E. Ekberg, Characterization of indoor sources of fine and ultrafine particles: A study conducted in a full-scale chamber, Indoor Air 15 (2) (2005) 141–150, http://dx.doi.org/10.1111/j.1600-0668.2005.00332.x.

[33] S.C. Lee, B. Wang, Characteristics of emissions of air pollutants from mosquito coils and candles burning in a large environmental chamber, Atmos. Environ. 40 (12) (2006) 2128–2138, http://dx.doi.org/10.1016/j.atmosenv.2005.11.047.

[34] J. Pagels, A. Wierzbicka, E. Nilsson, C. Isaxon, A. Dahl, A. Gudmundsson, E. Swietlicki, M. Bohgard, Chemical composition and mass emission factors of candle smoke particles, J. Aerosol Sci. 40 (3) (2009) 193–208, http://dx.doi.org/10.1016/j.jaerosci.2008.10.005.

[35] E. Géhin, O. Ramalho, S. Kirchner, Size distribution and emission rate measurement of fine and ultrafine particle from indoor human activities, Atmos. Environ. 42 (35) (2008) 8341–8352, http://dx.doi.org/10.1016/j.atmosenv.2008.07.021.

[36] M.A. Torkmahalleh, I. Goldasteh, Y. Zhao, N.M. Udochu, A. Rossner, P.K. Hopke, A.R. Ferro, $PM_{2.5}$ and ultrafine particles emitted during heating of commercial cooking oils, Indoor Air 22 (6) (2012) 483–491, http://dx.doi.org/10.1111/j.1600-0668.2012.00783.x.

[37] B. Jones, G. Phillips, C. O'Leary, C. Molina, I. Hall, M. Sherman, Diagnostic barriers to using $PM_{2.5}$ concentrations as metrics of indoor air quality, in: 39th AIVC Conference: 7th TightVent & 5th Venticool Conference. Ghent, Belgium, 2018, pp. 404–413.

[38] W. Ott, A.C. Steinemann, L.A. Wallace, in: W.R. Ott, A.C. Steinemann, L.A. Wallace (Eds.), Exposure Analysis, CRC Press, Boca Raton London, 2007.

[39] MATLAB Version 9.1.0.441655 (R2016b), The Mathworks, Inc., Natick, Massachusetts, 2016.

[40] I. Hughes, T.P.A. Hase, in: I.G. Hughes, T.P. Hase (Eds.), Measurements and their Uncertainties : A Practical Guide to Modern Error Analysis, Oxford University Press, Oxford, 2010.

[41] BSI, BSEN 12341:2014 Ambient air. Standard Gravimetric Measurement Method for the Determination of the PM_{10} or $PM_{2.5}$ Mass Concentration of Suspended Particulate Matter, Report, BSI, 2014.

[42] R.-T. Jiang, V. Acevedo-Bolton, K.-C. Cheng, N.E. Klepeis, W.R. Ott, L.M. Hildemann, Determination of response of real-time SidePak AM510 monitor to secondhand smoke, other common indoor aerosols, and outdoor aerosol, J. Environ. Monit. 13 (6) (2011) 1695–1702, http://dx.doi.org/10.1039/C0EM00732C.